PHYSICAL REVIEW B VOLUME 55, NUMBER 15 15 APRIL 1997-I

Band structure and optical properties of HgI_2

A. K. Solanki, Arti Kashyap, T. Nautiyal, and S. Auluck
Department of Physics, University of Roorkee, Roorkee 247 667, India

M. A. Khan
Institut de Physique et Chimie des Materiaux de Strasbourg, Universite Louis Pasteur, 4 rue Blaise Pascal, 67070 Strasbourg, France

(Received 10 October 1995; revised manuscript received 26 December 1996)

We have used the linear muffin-tin orbital–atomic sphere approximation method to calculate the band structure of red HgI_2. Our results are in excellent agreement with the self-consistent Korringa-Kohn-Rostoker calculation of Turner and Harmon. Using our self-consistent potential, we have calculated the anisotropic frequency-dependent dielectric function. This dielectric function is in agreement with the experimental data. We compare our calculations with those reported by Chang and James using an empirical nonlocal pseudopotential. [S0163-1829(97)11716-7]

INTRODUCTION

The electronic properties of HgI_2 have been a subject of recent theoretical studies. Mercuric iodide crystallizes in a tetragonal structure and has a measured band gap of 2.13 eV at 30 °C,[1] thus giving it a red appearance. It undergoes a transformation at 127 °C to an orthorhombic structure which persists upto its melting point of 259 °C. The yellow color of the orthorhombic phase suggests a decrease in the band gap of about 10%. As a result of the large atomic masses of the constituent atoms ($Z=80$ for Hg and $Z=53$ for I), HgI_2 has a high stopping power for photons. Its high bulk resistivity ensures low dark current during detector operation and a high photosensitivity so that the number of generated electron-hole (e-h) pairs is proportional to the incident photon energy. This makes HgI_2 well suited for x-ray and γ-ray spectroscopies. Although such applications have been amply demonstrated, there are problems associated with the small hole mobility (at RT and along c axis). It is natural to understand these properties on the basis of band-structure calculations.

There have been three recent band-structure calculations on HgI_2.[2–4] Yee, Sherohman, and Armantrout[2] have reported such a calculation. This was performed using an empirical pseudopotential. However, the calculations were done with an incorrect body centered tetragonal structure. Moreover, these calculations were nonrelativistic and also did not allow for charge transfer. More recently Chang and James[3] (CJ) have improved upon this calculation by using an empirical nonlocal pseudopotential (where the energy gap has been adjusted to the experimental value). Spin-orbit interaction has been included using first-order degenerate perturbation theory to save on computer time. CJ have calculated the electron and hole effective masses and the complex dielectric function. These are in agreement with the experimental data. The only scalar-relativistic self-consistent calculation has been performed by Turner and Harmon (TH) using the Korringa Kohn Rostoker (KKR) method where the final determination of band structure, incorporating spin-orbit coupling, was done using the linear augmented plane wave (LAPW) method. The switch over from KKR to LAPW, was a matter of convenience, since given the same potential the two methods yield essentially identical results. The band structures of CJ and TH are very similar. The TH calculations yield a band gap of 0.5 eV [this is expected in a local density approximation (LDA) calculation which are known to underestimate band gaps by as much as 50%] whereas in the CJ calculations the band gap is adjusted to the experimental value. Both calculations yield electron/hole masses that are in agreement with each other and with the experimental data.

Earlier interest in the optical properties of HgI_2 has been primarily to understand the hydrogenlike exciton series ($n=1,2$ states) near the fundamental edge which manifest themselves in absorption, reflectivity, photoconductivity, and luminescence.[5–10] Although there have been numerous studies of these, the frequency-dependent dielectric function has been neglected. The only calculation of the frequency-dependent complex dielectric function $\varepsilon(\omega)$ has been done using the empirical pseudopotential method (EPM). The good agreement with the recent data of Anedda, Grilli, Guzzi, Rega, and Serpi[9] has spurned us towards attempting a calculation of $\varepsilon(\omega)$ using the potential $V(r)$ from a self-consistent calculation. We report such a calculation in this paper.

METHOD OF CALCULATION

We have used the scalar relativistic linear muffin-tin orbital (LMTO) method within atomic sphere approximation (ASA) including the combined correction terms.[11,12] It has now been well established that this method gives the frequency-dependent dielectric function that is in agreement with the experiment not only for metals but also for intermetallic compounds.[13–15] The crystal structure of HgI_2 is tetragonal with $a=4.361$ Å and $c=12.450$ Å.[16] Since c/a is large, the structure is fairly open (i.e., packing fraction is small). The accuracy of band-structure methods based on the MT approximation is the maximum, when the packing fraction is highest. TH have achieved this by introducing 10 empty spheres. This results in a packing fraction of 60.65%, thus making it amenable to a MT based band-structure cal-

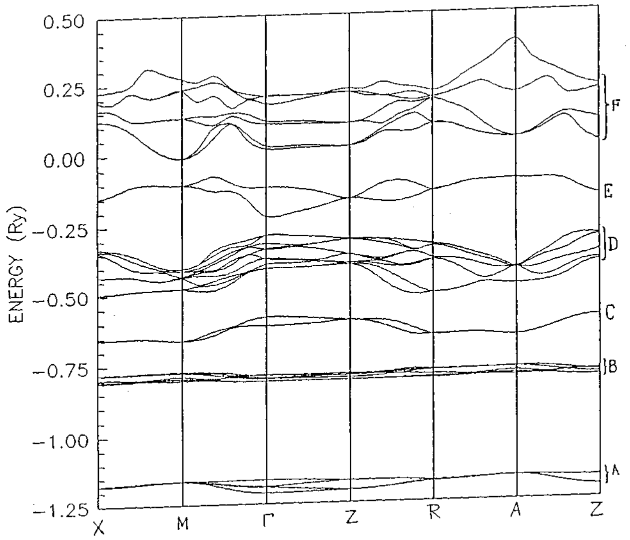

FIG. 1. Band structure of HgI_2 (*spd* calculation).

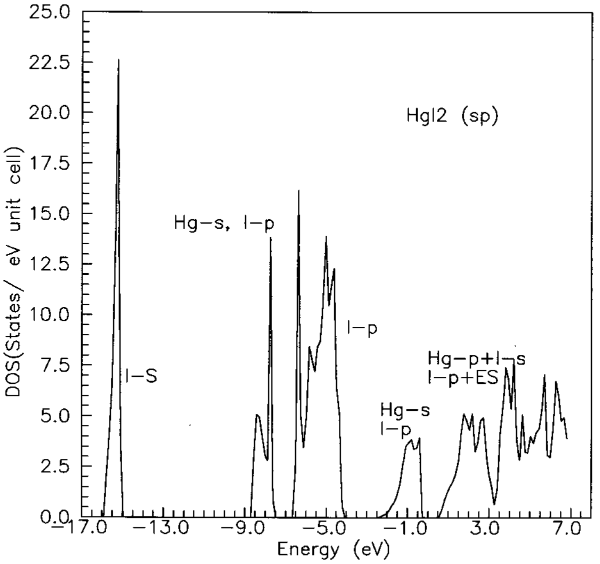

FIG. 2. Total density of states in states/eV/unit cell for the *sp* calculation (with marking of the major contributions to the different peaks).

culation. We have used the positions of the ES's as given by TH. The tetragonal unit cell now have 16 atoms (Hg-2, I-4, ES-10). The position of 2 Hg atoms are (0,0,0; 0.5, 0.5, 0.5) and 4 I atoms are $(0,0.5,u;\ 0.5,0,-u;\ 0,0.5,u+0.5,$ and $0.5,0,0.5-u)$ with $u=0.139$. We have expanded the wave function in two ways. (i) The valence configuration for Hg is taken to be $6s2$. The wave functions are expanded to include *s* and *p* states. We call this *sp* calculation. (ii) The valence configuration for Hg is taken to be $5d10\ 6s2$. The wave functions are expanded to include *s*, *p*, and *d* states. We call this *spd* calculation. In both calculations the I valence configuration is $5s2\ 5p5$. The calculations were done using 75 k points in the irreducible Brillouin zone (IBZ). Brillouin zone integrations are done using the tetrahedron method. We have used the von Barth–Hedin exchange correlation potential.[17] The results of (i) are directly comparable with the pseudopotential calculations of CJ and that of (ii) with the KKR calculation of TH. The CJ work shows that the inclusion of spin-orbit coupling does not have any significant effect on the band structure except that the double degeneracy is lifted and the energy gap is reduced by a few tenths of an eV.

BAND STRUCTURE AND DENSITY OF STATES

The band structure for the *spd* calculation is shown in Fig. 1. The only difference between this and the *sp* band structure is the presence of the Hg *d* states. We shall later discuss the differences between these two band structures. Our band structure looks similar to the TH and CJ calculations. All the calculations give bands that are bunched in groups with gaps between these groups. We attribute the minor differences to the fact that both TH and our calculations use the muffin-tin approximation along with expressing the wave function in terms of atomiclike states whereas CJ have used plane-wave-like states in the pseudopotential calculation. We believe that self-consistency will also play an important role here.

Consider first the density of states (DOS) in the *sp* calculation (Fig. 2). We find a sharp peak occurring around -15.2 eV arising from I-*s* and a broad structure extending from -6.4 to -4.4 eV arising from I-*p* states. We also find significant contributions to the total density of states (DOS) coming from the Hg-*s* and I-*p* states at -8.2 and -0.8 eV (E_F, as measured from the top of the valence band, is -4.0 eV). The ES's do not make any significant contribution except around 1.5 and 2.4 eV. The major contributions to the DOS from different atoms are shown in Fig. 2. These results are in agreement with the work of TH (if we ignore the Hg-$5d$ states), as well as with the work of CJ. TH identify the various structures in the total DOS as I-$5s$ (-9.5 eV), Hg-$6s$ and I-$5p$ (-1.4 and 5.4 eV), I-$5p$ (0.0 to 2.7 eV), while CJ obtain I-$5s$ (-11.0 eV), Hg-$6s$ and I-$5p$ (-4.5 and -3.0 eV), and I-$5p$ (-2.4 to 0.0 eV). The Fermi level is at 3.5 eV for the TH calculation and zero for the CJ calculation. Our *sp* calculation gives an energy gap of 1.67 eV, compared to the experimentally measured value of 2.37 eV. TH obtained a gap of 0.52 eV while CJ have empirically adjusted the gap to the experimental value. The *spd* DOS is shown in Fig. 3. The DOS looks similar (although structure is broadened) to the *sp* DOS except having a large peak around -8.7 eV arising from the Hg-*d* states. The DOS is in good agreement with the TH calculations both in terms of the height of the peaks and their location. The *spd* calculations demonstrate the importance of *sd* hybridization which has broadened the Hg-*s* and I-*p* states by about 1.1 eV and thereby reduced the energy gap. The major contributions to the total DOS come from Hg-*d* states, I-*s* and I-*p* states as marked in Fig. 3. The total DOS has many structures (the E_F is at -4.1 eV): a peak around -15.9 eV arising from the I-*s* states, structures around -8.7 and -1.6 eV arising form the Hg-*d* states, a broad structure around -6.8 to 3.8 eV arising from Hg-*s*, I-*s*, and I-*p* states, a structure around -10.9 eV arising from the I-*p* states and structures around 0.8 to 3.4 eV arising from the ES states. The relative positions of the peaks are in agreement with TH calculations. In the *spd* calculation the energy gap is 0.95 eV

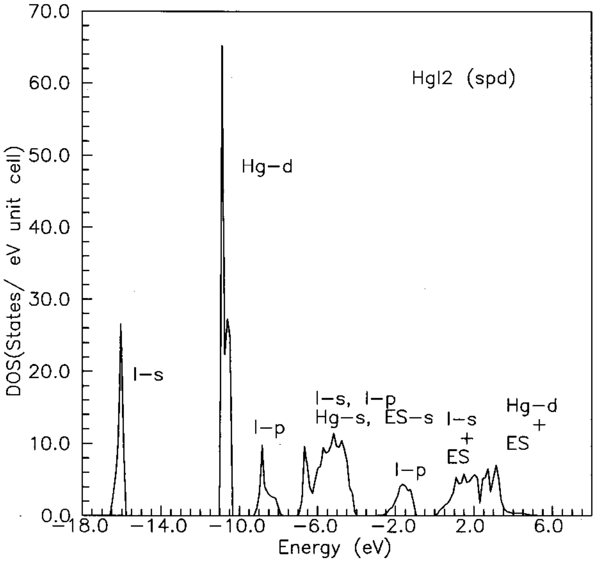

FIG. 3. Total density of states in states/eV/unit cell for the *spd* calculation (with marking of the major contributions to the different peaks).

compared to 0.52 eV obtained by TH. Relativistic effects will reduce our gap by a few tenths of an eV thereby approaching the value of TH. These gaps are smaller than the experimental gap. Such discrepancies are expected in a LDA calculation which is known to underestimate gaps by as much as 50%.

OPTICAL PROPERTIES

The calculation of the optical properties of solids is beset with numerous problems. The quantity of central importance is the dielectric function. It is complex and a tensor. For cubic systems there is only one component to be calculated, i.e., ε_{XX}. For hcp/tetragonal systems we have to calculate two components $\varepsilon_{\parallel}$ and $\varepsilon_{\perp}$ corresponding to electric field parallel and perpendicular to the c axis. The dielectric function is normally calculated in the random phase approximation (RPA). Calculations of the dielectric function involve the energy eigenvalues and the electron wave functions. These are natural outputs of *ab initio* band-structure calculations. We have thus performed calculations of the dielectric function of HgI_2 using the standard RPA expressions.[13,14]

The summation over the Brillouin zone is calculated using a linear interpolation on a mesh of uniformly distributed points, i.e., the tetrahedron method. We have done calculations using 126 k points in the IBZ.

To bring out the high energy structure more clearly it is sometimes instructive to plot the optical conductivity $\sigma(\omega)[(\omega/4\pi)\mathrm{Im}\,\varepsilon(\omega)]$. However, since the experimental data is on the dielectric function in the range 0–10 eV we have decided not to show our results of the optical conductivity. The calculated dielectric functions for the *sp* calculation are shown in Fig. 4. We see that the anisotropy in the calculated $\mathrm{Im}\,\varepsilon_{\parallel}(\omega)$ and $\mathrm{Im}\,\varepsilon_{\perp}(\omega)$ is rather small. This is all the more surprising considering the large c/a ratio. Both the $\mathrm{Im}\,\varepsilon(\omega)$ show two main peaks centered around 4.2 and 6.8 eV and a weak broad maxima around 10.6 eV.

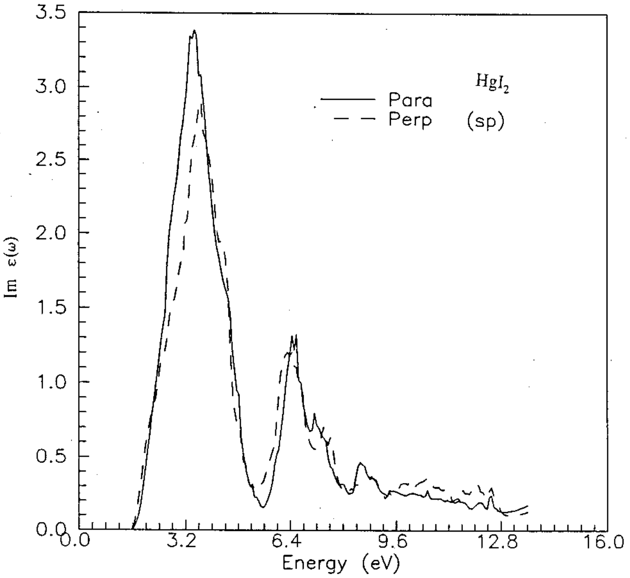

FIG. 4. $\mathrm{Im}\varepsilon_{\parallel}(\omega)$ and $\mathrm{Im}\varepsilon_{\perp}(\omega)$ for the *sp* calculation.

The position of the two main peaks is in agreement with the experimental data as also the ratio of the peak heights. However, the magnitude of the peaks heights is underestimated by a factor of 3 compared to the experimental data.

The results of the *spd* calculation are shown in Fig. 5. Once again there are two main peaks centered around 4.2 and 6.8 eV. The calculated peak heights are about the same for $\mathrm{Im}\,\varepsilon_{\perp}(\omega)$ while for $\mathrm{Im}\,\varepsilon_{\parallel}(\omega)$ the higher energy peak height is larger. This latter fact is in disagreement with the experimental findings.[9] In contrast to the *sp* calculation the peak heights are larger and closer to the experimental values. Also in agreement with the data and in contrast with the *sp* calculation, the *spd* calculation shows more structure in the form of minor peaks. The *spd* calculation shows more anisotropy in the calculated dielectric functions compared to

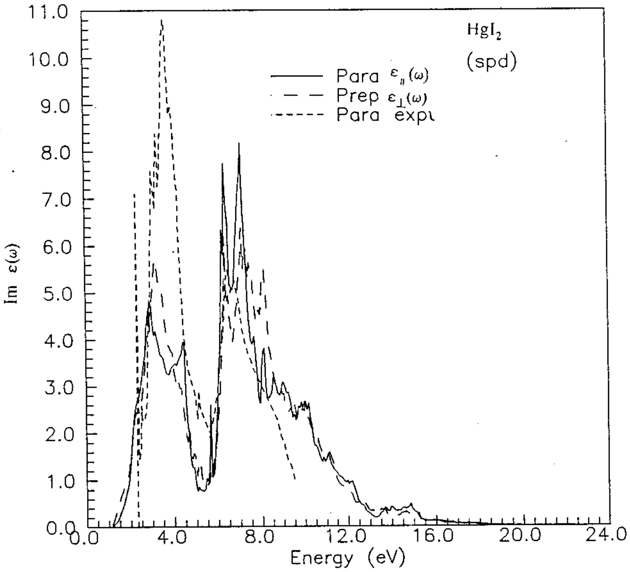

FIG. 5. $\mathrm{Im}\varepsilon_{\parallel}(\omega)$ and $\mathrm{Im}\varepsilon_{\perp}(\omega)$ for the *spd* calculation. The experimental $\mathrm{Im}\varepsilon_{\parallel}(\omega)$ of Anedda *et al.* (Ref. 9) is also shown.

the sp calculation. This could be due the anisotropy of the d wave functions. The sp wave functions are more isotropic. It would be nice if experiments are done for both Im $\varepsilon_{\perp}(\omega)$ and Im $\varepsilon_{\parallel}(\omega)$ to bring out this anisotropy more clearly and to identify the minor structures.

It would seem interesting to see if the structures in $\varepsilon(\omega)$ can be explained by our band structure. The band structure shown in Fig. 1 reveals that the bands are bunched together in groups. We label these as A–F. Starting from the low energy side, the first group (A) is mainly the I-s states. Group (B) is the Hg-d states and (C) is the I-p states. The broad bunch of bands below the fermi level (D) are the I-s and Hg-s states. (E) comprises the antibonding I-p states and (F) comprises the I-s, Hg-d, and ES states. The Fermi level lies between D and E. The first broad structure around 4 eV in Im $\varepsilon(\omega)$ comes from the transitions between D and E. The next sharp peak around 5.5 eV may be attributed to transitions from C to E. The peak around 7 eV may arise from D to F transitions. On the high energy side the transitions from B to E and A to E can account for the 10 and 15 eV peaks. Since all the structures in DOS are admixtures of different angular momentum and atomic species, it is not possible to identify the exact nature of these optical transitions.

CONCLUSIONS

We have studied the band structure and optical properties of HgI_2 using the LMTO-ASA method. From our calculations, we observe that band gap and dielectric function are nicely represented within the limitations of LDA. Our calculations give a band gap of 1.37 eV (from sp calculation) and 0.95 eV (for spd calculation) compared to the experimental value of 2.13 eV. A recent KKR calculation yields a value of 0.52 eV. We expect that relativistic effects will reduce our gap by a few tenths of an eV. Our calculation show that the effect of matrix elements is very significant and necessary to explain the experimental data. We also find that a better representation of wave function (i.e., spd) leads to a improved agreement with the experiment, although it gives a smaller band-gap. Naturally going to a $spdf$ representation should yield even better values for Im $\varepsilon(\omega)$. In the case of HgI_2 the calculations would require a lot of computer time. We have, therefore, done calculations for the elemental semiconductor silicon and find that there is not much change (less than 10%) in Im $\varepsilon(\omega)$ when going from a spd wave function to a $spdf$ wave function. Thus the LMTO-ASA method with a spd wave function gives the frequency-dependent dielectric function that agrees well with the experimental data.

ACKNOWLEDGMENTS

The calculations were done at the New Computing Facility (NCF) and at the Physics Department Computing Facility (PHYCF). We are thankful to them. We are grateful to the Council of Scientific and Industrial Research (CSIR) for financial support in the form a research grant and research associates. We would like to thank Sangeeta Sharma for her help in the final stages of this work.

---

[1] See M. Piechotka and E. Kaldis (unpublished) for review of the physical properties of HgI_2.

[2] J. H. Yee, J. W. Sherohman, and G. A. Armantrout, IEEE Trans Nucl. Sci. **NS-23**, 17 (1976).

[3] D. E. Turner and B. N. Harmon, Phys. Rev. B **40**, 10 516 (1989).

[4] Yia-Chung Chang and R. B. James, Phys. Rev. B **46**, 15 040 (1992).

[5] B. V. Novikov and M. M. Pimonenko, Fiz. Tekh. Poluprovodn. **4**, 2077 (1970) [Sov. Phys. Semicond. **4**, 1785 (1970)].

[6] K. Kanzaki and I. Imai, J. Phys. Soc. Jpn. **32**, 1003 (1972).

[7] A. Anedda, F. Raga, E. Grilli, and M. Guzzi, Nuovo Cimento **38**, 439 (1977).

[8] P. D. Bloch, J. W. Hodby, C. Schwab, and D. W. Stacey, J. Phys. C **11**, 2579 (1978).

[9] A. Anedda, E. Grilli, M. Guzzi, F. Raga, and A. Serpi, Solid State Commun. **39**, 1121 (1981).

[10] T. Goto and A. Kasuya, J. Phys. Soc. Jpn. **50**, 520 (1980).

[11] O. K. Andersen, Phys. Rev. B **12**, 3060 (1975).

[12] H. L. Skriver, *The LMTO Method* (Springer, New York, 1984).

[13] C. Koenig and M. A. Khan, Phys. Rev. B **27**, 6129 (1983).

[14] M. Alouani, J. M. Koch, and M. A. Khan, J. Phys. F **16**, 473 (1986).

[15] M. A. Khan, Arti Kashyap, T. Nautiyal, and S. Auluck, Phys. Rev. B **48**, 16 974 (1994); A. K. Solanki, Arti Kashyap, T. Nautiyal, S. Auluck, and M. A. Khan, Solid State Commun. **94**, 1009 (1995).

[16] G. A. Jeffrey and N. Vlasse, Inorg. Chem. **6**, 396 (1967).

[17] U. von Barth and L. Hedin, J. Phys. C **5**, 1629 (1972).